

A New Optimal Sensor Location Method for Double-curvature Arch Dams: A Comparison with the Modal Assurance Criterion (MAC)

Amir Meysam Giahi^{1*}, Jafar Asgari Marnani^{1*}, Mohammad Sadegh Rohanimanesh¹, Hassan Ahmadi²

¹ Department of Civil Engineering, Faculty of Civil and Earth Resources Engineering, Central Tehran Branch, Islamic Azad University, 1955847781 Tehran, Iran

² Department of Civil Engineering, Roudehen Branch, Islamic Azad University, 3973188981 Roudehen, Iran

* Corresponding author, e-mail: j_asgari@iauctb.ac.ir; ami.giahi.eng@iauctb.ac.ir

Received: 09 February 2023, Accepted: 21 September 2023, Published online: 06 November 2023

Abstract

Determining the optimal location of sensors in order to identify modal parameters in large structures such as dams is one of the most important and widely used topics in damage detection and health monitoring of structures. In this research, the modal parameters including the natural frequency and mode shape of two arched concrete dams have been calculated using the finite element method for healthy and damaged dams. The reduction of the elastic modulus of concrete in different parts and percentages has been used as the degree of damage. Then, using the modal confidence criterion (MAC) method, the optimal location of the sensors is determined, then the results of this method are compared with the new method. The results show that in both dams, the new method matches the MAC method with 90% accuracy. This new method is a fast and suitable measure to determine the optimal location of sensors in arched concrete dams.

Keywords

structural health monitoring, concrete arch dam, modal characteristics, modal assurance criterion, optimal sensor location

1 Introduction

Historically, the science of structural health monitoring evolved simultaneously with the development of engineering structures, utilizing various methods for measuring and optimizing the performance of the structural system. For instance, in the early nineteenth century, the sound produced by a hammer striking a railway track was regarded as a criterion for diagnosing damage to or the health of this type of system [1].

Developed various techniques have been developed regarding rotating machinery to monitor the structural health of this type of structure using vibration measurement [2]. Since then, various structural systems such as buildings, bridges, among others, have been investigated, and various methods have been developed in this regard.

Since the dawn of humanity, the construction of dams for flood control, the storage of drinking and agricultural water, and the maintenance of electricity, among other purposes, has been considered. Historically, depending on

the need of local communities, an effort has been made to construct a dam, barrage, or offtake. These types of structures were primarily constructed for water maintenance and storage.

In some regions, dam building has been practiced to raise the water level and direct it to appropriate locations for agricultural or other civil purposes and divert the flow direction of rivers. Water has long been regarded as a valuable resource in Iran, both urban and rural, due to water scarcity and unique climate conditions. This issue is evident in the construction and development of dams in Iranian communities and the preservation of monuments from previous eras that demonstrate the value of water to them. It is self-evident that any damage to vast structures and infrastructure deprives communities of their benefits, imposes significant financial losses, may result in irreversible fatalities and severe damage to intellectual and environmental capital.

Considering that dams are critical strategic and essential structures for any country, their safety and performance are essential in designing novel structures and monitoring their health during operation. Among the various concrete dam types, arch dams are the most critical, both economically and structurally. Arch dams, particularly when compared to concrete gravity dams, are significantly more cost-effective and can be built faster. They do, however, require high-quality concrete in higher-quality and more expensive forms. Additionally, they necessitate a more involved design process [3].

The use of structural modal parameters in structural health monitoring dates to the late 1970s. Initially, changes in the system's natural frequency were examined in order to detect structural damage. Cawley and Adams's [4] research is an example of relevant work on this subject. Rather than examining the effect of damage on frequency changes, some researchers examined the changes in mode shapes caused by structural damage. For example, West introduced the Modal Assurance Criterion (MAC) concept and attempted to establish a mathematical relationship between the analytical mode shapes and the experimental results. Additionally, some researchers investigated alternative methods for detecting damages, such as mode shape characteristics [5].

Ghasemi et al. [6] proposed a Monte-Carlo simulation-based approach for accounting for uncertainty effects when developing a probabilistic surrogate model. In this study, the model was updated using the Enhanced Ideal Gas Molecular Movement (EIGMM) algorithm, and the proposed method was applied to truss structures. In summary, this research established that the proposed technique for detecting structural damage might provide superior performance while requiring less computational effort than the direct finite element method.

Zhu et al. [7] used the quantum genetic algorithm to determine the optimal location of sensors on a concrete dam. Their primary objective was to ascertain the structural modal parameters. They accomplished this by presenting an effective and independent criterion using the Modal Strain Energy (MSE) method to determine the optimal location of sensors on the upstream face of high concrete arch dams.

Chen et al. [8] proposed a combined method for determining the optimal location of sensors to obtain the dynamic response of hydraulic structures. They combined the modal assurance criterion (MAC) method with the modal strain energy method (MSE) to introduce a new approach for

mitigating the sensors' initial location effect. This study conducted simulations of an arch dam using 20 sensors and the structure's first six vibration modes. Additionally, this study examined the proposed method's advantages and disadvantages compared to other methods such as the MAC, Modal Kinetic Energy Criterion, Fisher Information Matrix, and Root-Mean Square Error Criterion.

Esmailzadeh et al. [9] conducted a study on a concrete gravity dam and used the MAC method to determine the location of damage caused by the Hilbert-Hung transfer technique to the concrete gravity dam. They then introduced a relative frequency error parameter based on changes in the frequencies of damaged points. According to the proposed criterion, the results indicated that the precise length and location of damage in a concrete gravity dam could be determined.

Shi et al. [10] used a concrete dam as the case study and designed various dam sections by altering the dam body's constituent materials. They also conducted stress analysis for six different states based on the gravity dam's elasto-plastic behavior. The models used in their analyses were the Concrete Damaged Plasticity (CDP) model, the Lagrangian Finite Element Model (FEM), and the surface-to-surface contact model. Finally, a comparison study was conducted, and a design for the combined dam structure was optimal.

Zhang et al. [11] conducted extensive research on the location of damage to the concrete dam and concluded that the seismic damage diagnosis system could be used to monitor seismic damage by recording the dynamic stress history. Furthermore, this feature was used to determine the damage distribution within the dam body's affected area.

Hamidian et al. [12] presented a combined wavelet method for damage diagnosis in 2D and 3D irregular continuum structures. They incorporated a neural network model and detected the damage location based on the displacement and stress outputs from the analysis of the damaged structures. The results obtained from the analysis were compared before and after the damage for detecting damages in the presented method. The applied method was highly effective at detecting damaged areas within the structure.

Gomez and Purcino Pereira [13] demonstrated how to optimize a Fisher Information Matrix using the Firefly Algorithm (FIMFA). The optimized sensors effectively detected damage in this method, particularly in large and complex structures. They demonstrated that the FIMFA method could detect damage optimally in various SHM applications in complex structures.

Honarbaksh et al. [14] conducted numerous studies on different structures, including a truss, to identify sensitive points. The assumed damage in the members was modeled in this study by decreasing the stiffness of the corresponding element. A truss was subjected to various damage scenarios to evaluate the proposed methods' efficacy. The results demonstrated the effectiveness of the methods mentioned above. Both methods for detecting damage in the truss structure and the two-dimensional frame could accurately determine the location and extent of damages [14].

In 2007, Cotae et al. [15] performed optimization of sensor locations and sensitivity analysis to monitor health using minimal interference algorithms. The general optimization of sensor locations and sensitivity analysis based on minimizing the interference caused by wireless communication between sensors in the presence of additional white Gaussian noise (AWGN) has been studied. In this study, when the data measured for sensitivity analysis by AWGN is variable, we obtain the necessary conditions under which the number of sensors and the optimal placements of the sensor remain unchanged. Theoretical results are confirmed by simulations that provide details of numerical implementations. Li et al. [16] found the optimal placement of thermal sensors for the Shanghai Bridge. Yi et al. [17] found the optimal placement of sensors for high-rise buildings.

Vegrzyn and Fonseca [18] in 2021 studied the optimization of sensor locations to improve the worst detection performance of sensor detection systems. Consider designing a sensor system to detect the emitter in an unknown location. For this scenario, the sensors have been placed in a typical network pattern. This paper shows that we can improve the worst-case detection mode on a network pattern by optimizing sensor locations. Using the Torczon local search algorithm, our results show that this algorithm can improve the worst-case scenario by up to 23% in the given scenario.

In 2000, Shi et al. [19] studied the placement of an optimal sensor to detect structural damage. A method for optimizing sensor locations and detecting damage in a structure using the information collected in this study has been presented. Unlike most available methods, sensor locations are prioritized based on their ability to determine the location of structural damages based on the specific sensitivity vector method. This is in line with the requirements for localization of structural damage. Only a small subset of total structural degrees of freedom has been measured, and the incomplete states resulting from these optimized

sensor locations are used to determine the location of structural damage. Numerical examples and test results show that this method is effective for detecting structural damage directly using optimal and incomplete test modes.

In 2020, Han et al. [20] performed a statistically optimized neural network model and its application to monitor deformation and predict failure on concrete gravel dams. Monitoring the deformation and safety function of CFRDs is important in ensuring the safety of human life and property in downstream areas. A new predictive model for horizontal displacement of CFRDs, the statistically optimally propagated neural network model, combining a statistical model and a backpropagation neural network model (BPNN), located at Dez Dam, Yunnan Province, southwest China was presented. Accordingly, an improved statistical model for the horizontal displacement of concrete-face rockfill dams (CFRDs) has been proposed.

In 2021, Altunisik et al. [21] have studied the optimal placement of sensors and the capabilities of this method to identify the dynamic properties of arch dams. For this purpose, a prototype of the arch dam is made in laboratory conditions. The Barakeh Arch Dam, located on the Ceyhan River in the Ottoman city, is one of the tallest arch dams built in Turkey and has been selected for field research. Ambient vibration tests are performed using the initial locations of Candida sensors at the beginning of the study. Advanced frequency amplitude analysis methods and stochastic spatial identification methods are used to derive experimental dynamic properties. Then, the measurements are repeated according to the optimal sensor locations of the dams. These sites are identified using the effective independence method. To determine the optimal sensor locations, target state matrices obtained from vibration tests of the selected dam environment with a large number of accelerometers are used. The dynamic properties of each environmental vibration test are compared. It is concluded that the dynamic properties obtained from the initial measurements and those obtained from a limited number of sensors are compatible with each other. This situation shows that the optimal placement of sensors with effective independence method is useful for identifying the dynamic properties of arch dams.

In 2020, Gomes and Pereira [22] studied the optimization of sensor placement and damage detection in the body structure using the inverse and firefly algorithm. In this study, damages are identified by solving an inverse problem. An E190 fuselage model has been considered and the firefly algorithm (FA) has been used to solve the inverse

problem to identify structural damage (location and severity). This method is then solved on two main fronts: (1) direct problem using finite element analysis and (2) inverse problem by minimizing an objective function. For this purpose, the sensor optimization method is performed using Fisher information matrix (FIM). The results are compared according to the problem of sensor placement optimization. It has been noted that optimized sensors help to improve damage detection mainly for complex and large-scale structures. Optimal Damage Identification Process Using FIM-FA can extend to a wide range of SHM applications in complex structures. Therefore, traditional NDIs have many defects due to the complexity of large-scale structures as well as modern design structures, and if access to the structure is limited, it is not possible. Accordingly, a damage enhancement detection method has been developed to better manage measurement data to find structural changes (or damage) in complex aerospace structures.

In 2018, Gomes et al. [23] studied the optimization of sensor placement in vibrating multilayer composite panels. In this study, the optimal sensor placement optimization for structural health monitoring systems has been studied. Several sensor optimization techniques are used in the shell structure. The structure, a sheet of carbon fiber, was modeled by the finite element method (FEM) and then exposed to free vibration. Genetic algorithms (GA) are then used to determine the best sensor distribution to cover a certain number of low frequency modes. Numerical results show the overall efficiency of sensor delivery methods.

In 2019, Gomes et al. [24] conducted research on optimizing the multi-purpose sensor placement for SHM systems by considering the Fisher information matrix and interpolating the shape of the mode. Global multifunctional optimization of sensor locations for structural health monitoring systems has been studied in this research. First, a multilayer composite plate has been modeled using the finite element method (FEM) and placed in modal analysis. Then, multipurpose genetic (GA) algorithms are used to search for the optimal location of the sensors. Numerical issues arising from the selection of the optimal sensor configuration in structural dynamics are investigated. A method for optimizing multi-purpose sensor locations using data collected by the FIM and state shape interpolation has been presented in this paper. Sensor locations are prioritized according to their ability to locate structural damage based on the specific sensitivity vector method. The method proposed in this paper allows you to

distribute the acquisition points on a structure in the best possible way so that both more modal information and data can be obtained from minimum point interpolation for better modal reconstruction.

In 2020, Hernandez et al. [25] studied verifying of the finite element model of the bridge based on the vibration monitoring at different stages of construction. Modal parameters experimentally obtained for the second stage were used to update its corresponding FE model considering two scenarios, before and after the installation of the asphalt pavement. The results presented in this study demonstrated that a rigorous construction control is needed in order to effectively calibrate FE models during the construction process of segmental bridges.

In 2020, Mehboob et al. [26] studied on numerical study for evaluation of a vibration-based damage index for effective damage detection. An improved damage detection index for a structural component is proposed, using eigenvalues estimated by means of frequency domain decomposition and mode contribution subjected to ambient excitation. It is based on vibration measurements obtained from the acceleration data of a simple steel beam. Since the extraction of modal parameters involves practical limitations and, in general, it is difficult to obtain accurate results, therefore in the proposed method a derivative value of the time series acceleration response, termed modal contributing parameter (MCP), is used in combination with eigenfrequencies. The damage is indicated by element stiffness reduction (ESR). Different damage cases for various stiffness reduction values of 1% to 15% were investigated. Damage identification indices for every single damage and multiple damage cases were calculated. The modified MCP damage detection index showed a high index value, even for low-level damage with an element stiffness reduction of as low as 1% over the existing frequency drop and indices based on mode shape change. MCP index derived from the modal response, considering modal contributions to the entire structural response and eigenvalues for damage detection, improved overall sensitivity and reliability of index results. Both single and multiple cases of damage provided equally accurate results based on the MCP index value.

A review of the published research indicates that damage detection in concrete arch dams has received less attention. Most of studies on dam health monitoring have relied on collecting instrumentation data and developing statistical models for predicting likely damages. Examining the research conducted on damage detection revealed that the

methods examined primarily involved simple structural elements such as frames, beams, and trusses (which possess much more simple governing equations than those needed for a dam's behavior).

To this end, the following questions should be addressed: what is the optimal location on the arch dam body for collecting the most data from the structure's modal response, and how could the optimal location of sensors be determined through the interpretation of these data and the application of modal assurance criterion methods. The current research will address these questions by examining the detrimental effect on the modal characteristics of concrete arch dams. The numerical analysis method in the finite element software Abaqus was used to accomplish this goal. Finally, the optimal location for placing the sensors is determined by examining the corresponding results of the modal deformations in each mode using the modal assurance method.

Previous studies have proposed a variety of approaches to damage identification. However, the methodologies that need the installation of too many sensors at different positions are known to be costly and in need for careful and frequent inspections. In this study, mode shapes and arbitrarily imposed damages to different points of a dam were used to identify the most appropriate position for installing the sensor for the dam. Therefore, a novelty of this research comes in the face of presenting a simple equation that agrees well with the modal assurance criterion (MAC) method.

2 Ease of use assessment criterion

With the limitations inherent in measuring dynamic responses in systems with a high degree of freedom, such as concrete dams, where the necessary data for identifying structural parameters are not determined adequately, diagnosing the structure's health would be prone to errors and problems. For this purpose, a selection of the vibration measurement points would be addressed first.

By considering the importance of measuring a structure's vibration motions to determine its vibration modes, the question of where to place the sensors to obtain the most data and information about the structure is raised.

This study's criterion is based on the minimization of the modal assurance matrix (Min-MAC). The modal assurance criterion (MAC) is defined in terms of the MAC matrix's off-diagonal terms, such that a lower maximum value for the matrix's off-diagonal terms indicates greater linear independence of the measured modes.

3 Modeling

Two double curvature concrete arch dams were adopted for this study. The first model of a fictive arch dam with the corresponding foundation and reservoir, given by the ICOLD benchmark workshop formulators. The dam is a 220 meter double curved symmetric arch dam that is 430 m broad at the crest and 80 m at the bottom. The thickness at the center section varies from 8 m at the top, to 55 m at the base. The foundation model is 1000 m wide, 1000 m long and 500 m high with a straight river with the same geometry as the dam. The reservoir is 500 m long (that is approximately two times the dam height) with a constant cross section. The second dam considered was Berke Dam in Turkey. This dam is 201 m tall, making it one of the largest in Turkey. This project began in 1995, was completed in 1999, and has been in operation in 2001 under the supervision of Turkey's Agriculture Ministry (T.C. Tarım ve Orman Bakanlığı). This concrete arch dam is located in the Düziçi district of the Osmaniye region and built on the Ceyhan River. Berke Dam is the region's primary source of energy. This dam generates 1458689000 kWh (kilowatt-hours) of electrical energy, enough to supply power to 440000 people. Water storage capacity behind the Berke Dam could be increased to 427 million cubic meters, and the reservoir behind this dam covers an area of 8.7 square kilometers. For simplicity, DM1 names first Dam and DM2 names Berke Dam in this section.

The investigated model is a concrete double curvature arch dam selected for its geometric characteristics and dimensions based on Helgren's research [27]. Fig. 1 depicts the dam's plan and southern view. Additionally, Table 1 illustrates the mechanical properties of the concrete used to construct these dams.

The structure's finite element model was created using the 8-noded element C3D8R in the Abaqus software (Fig. 2). As can be seen, the element type chosen for integration is

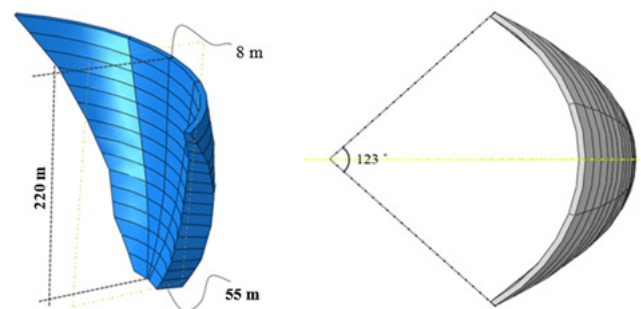


Fig. 1 Description of the model geometry corresponding to the concrete double curvature arch dam (a) plan, (b) Southern view (DM1)

Table 1 Properties of the studied dams

Properties	Value	Unit
Density	24	kN/m ³
Modulus of elasticity	27	GPa
Poisson's ratio	0.20	-

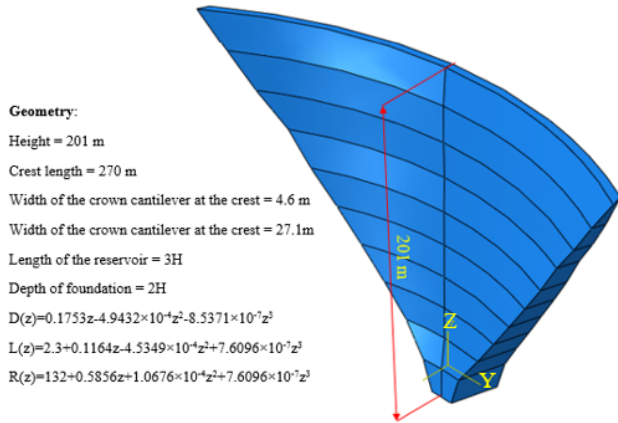


Fig. 2 Element used for the 3D finite element model of the concrete arch dam (DM2) [27]

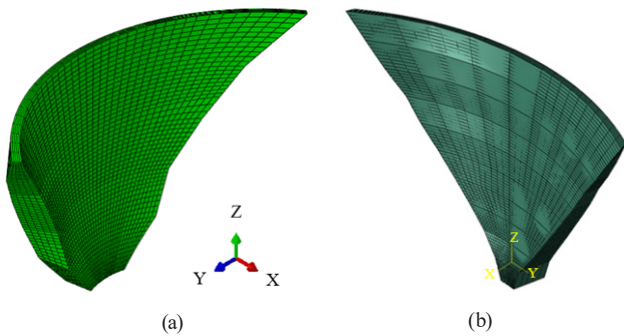


Fig. 3 The dam body meshing used in the studied double curvature arch dams' finite element model, (a) DMI, (b) DM2

a solid, 3D element with 8 Gauss points. Additionally, Fig. 3 depicts the dam meshing process using the standard 8-noded elements for the dam's body. Fig. 4 showed Berke Dam.

To analyze the dam, the transitional and rotational degrees of freedom are closed on the right and lower sides of the dam.



Fig. 4 The Berke Dam

In the foundation and sides of the dam, the support has been considered in fixed mode.

The dam was divided into three zones, as illustrated in Fig. 5, namely upper, middle, and lower. Each zone was assumed to have three damaged locations, with a total of nine damaged locations.

In this study, because damage reduces stiffness and softens the system, the damage is modeled as a decrease in the value of the modulus of elasticity. Three damage levels were used for this purpose: a 10%, 30%, and 50% reduction in the modulus of elasticity.

The dam structure was first subjected to a linear modal analysis to determine the healthy structure's modal characteristics. As previously stated, it is impossible to consider all vibration modes in the analysis of arch dam structures due to their extremely high degrees of freedom. As a result, the modes exerting the most significant influence on the modal structure responses should be identified. The modal participating mass ratio was used in this study to determine the system's more significant modes, as indicated in Table 2.

These mode shapes, along with their corresponding periods and natural frequencies, are depicted in Fig. 6.

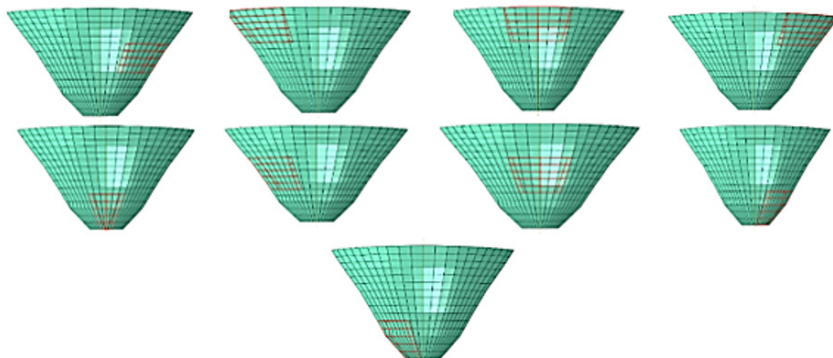


Fig. 5 Dividing the dam into different areas

The effective mode in each direction is identified using the vibrated mass values in the vibration modes. Thus, the mode of vibration in which the structure's largest mass vibrates can be designated as the effective vibration mode.

3.1 Verification

Helgren's research [27] from 2015 was used to validate the model. For modeling purposes in this study, a symmetrical concrete double-curvature arch dam with a height of 220

m was used. The dam spans 430 meters at its crest and 80 meters at its base. The dam measures 8 m in width at its crest and 55 m at its base, and its height is 220 m. Table 3 lists the properties of the material used in this dam.

The dam's applied loads are comprised of the dam's weight and the hydrodynamic force generated by the water in the dam reservoir. The modal analysis results for the first to ninth modes are presented in Table 4 for both the current study and Hellgren's work.

Table 2 The modal participating mass ratios

Number of Mode	Ux	sum(Ux)	Uy	sum(Uy)	Uz	sum(Uz)
1	1.74×10^{-7}	1×10^{-7}	3.13×10^{-9}	3×10^{-9}	0.091801	0.0918
2	0.24976	0.2497	0.004	0.0042	6.3×10^{-8}	0.0918
3	0.02955	0.2793	1.9×10^{-3}	0.0061	$4. \times 10^{-12}$	0.0918
4	0.22817	0.5075	1.78×10^{-2}	0.0240	$2. \times 10^{-10}$	0.0918
5	3.3×10^{-11}	0.5075	1.12×10^{-12}	0.0240	0.00623	0.098
6	9.2×10^{-12}	0.5075	1.14×10^{-10}	0.0240	0.15729	0.2553
7	0.03348	0.5409	7.09×10^{-3}	0.0311	3×10^{-10}	0.2553
8	0.00781	0.5488	1.29×10^{-1}	0.1599	5×10^{-12}	0.2553
9	0.0090	0.5578	4.26×10^{-1}	0.5858	4×10^{-11}	0.2553
10	5×10^{-9}	0.5578	5.85×10^{-10}	0.5858	0.02271	0.2780

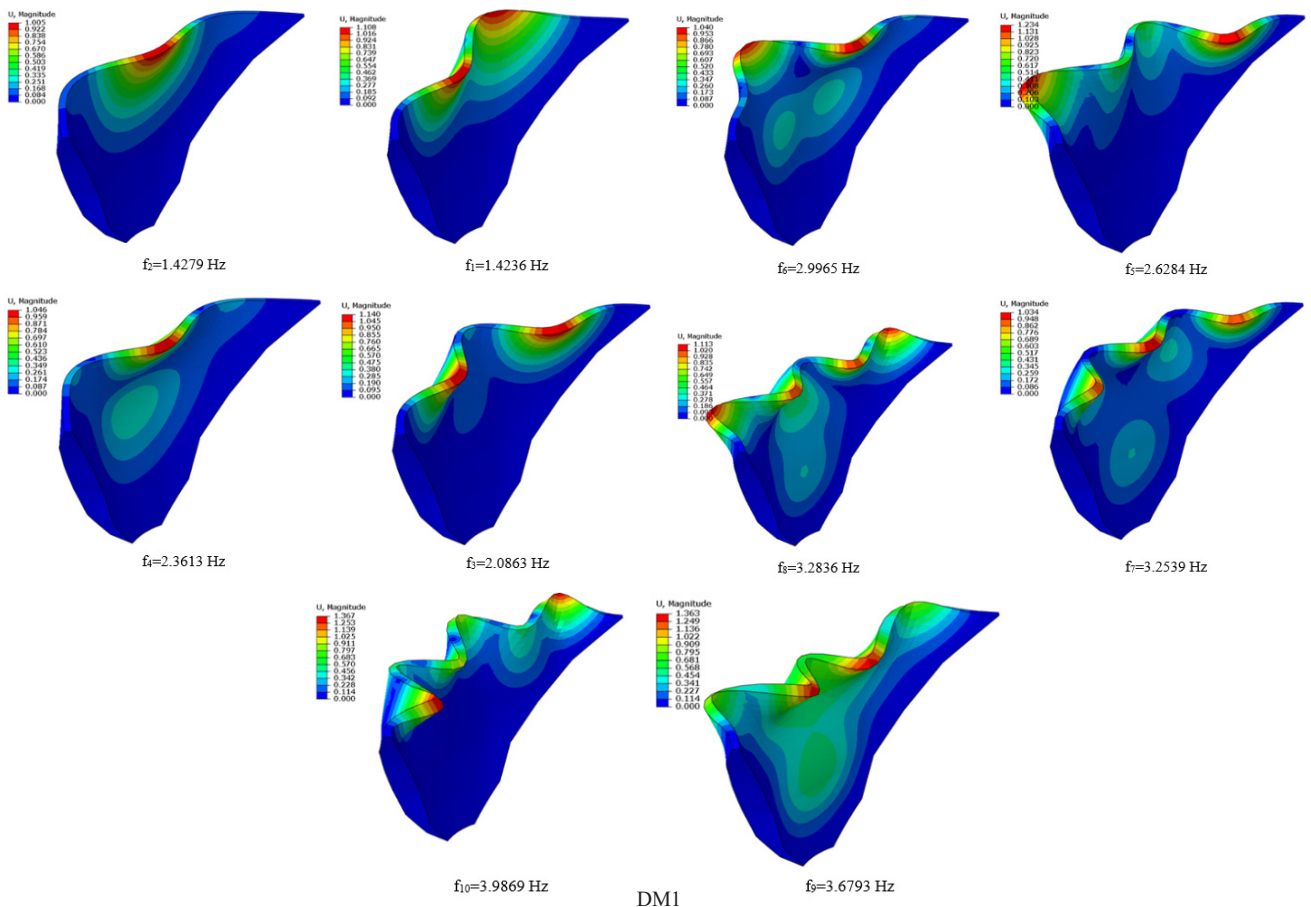
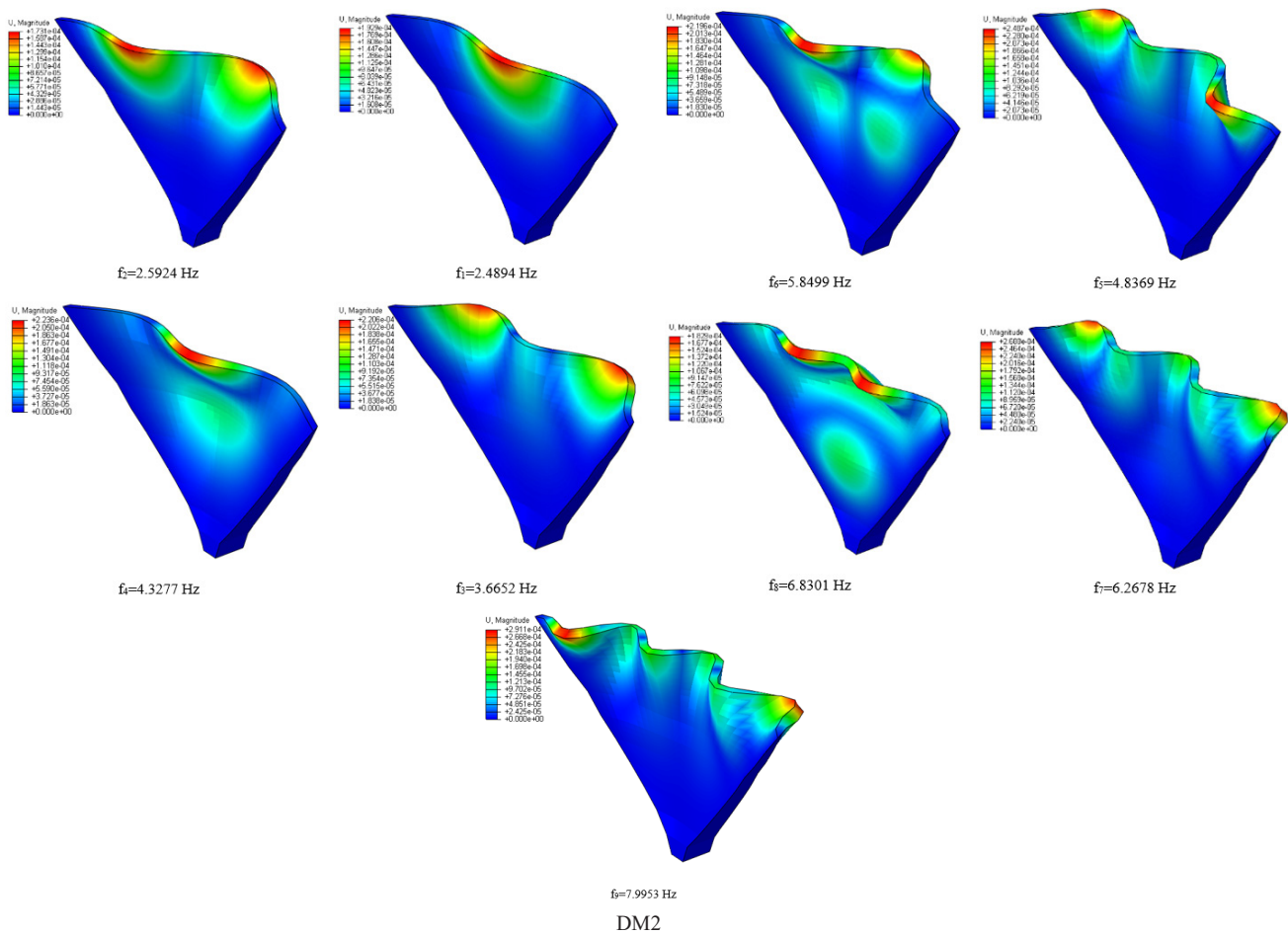


Fig. 6 Mode shapes affecting the dams under evaluation (continuation on the next page)



DM2
Fig. 6 Mode shapes affecting the dams under evaluation

Table 3 The studied dam's properties and the water stored behind it [27]

	Density [kg/m ³]	Poisson's ratio	Young/Bulk Modulus [GPa]
Arch dam	2400	0.2	27
Foundation	0	0.167	25
Water	1000	-	22

As illustrated in Table 4, the results of both models are highly compatible.

3.2 Investigated scenarios

Fig. 7 illustrates the assumed points for determining the optimal location of the sensors and the studied scenarios.

4 Modal Assurance Criterion (MAC)

The modal assurance criterion (MAC) is a widely used technique for performing quantitative comparisons of modal vectors. This criterion illustrates the relationship between two distinct collections of modal shapes. This criterion is also used to evaluate the analytical and experimental modal vectors performance. The MAC coefficient

Table 4 Frequency modes of the studied dam DM1

Mode	DM1 (Hz)	Hellgren (Hz) [27]	percentage error
1	1.42	1.52	0.07
2	1.43	1.54	0.07
3	2.08	2.05	0.01
4	2.36	2.27	0.04
5	2.63	2.53	0.04
6	2.99	2.94	0.02
7	3.25	3.19	0.02
8	3.28	3.32	0.01
9	3.68	3.72	0.01
10	3.99	3.90	0.02

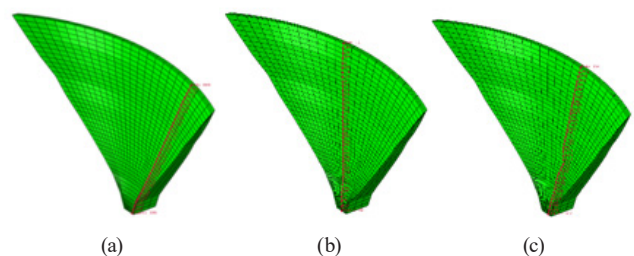


Fig. 7 Various scenarios for determining the optimal location for sensors; (a) First Scenario, (b) Second Scenario, (c) Third Scenario

is defined as the normalized scalar coefficient between two sets of vectors $\{\phi_A\}$ and $\{\phi_B\}$, and the equation used to calculate it is as follows [28–29]:

$$MAC_{ij} = \frac{\left| \{\phi_A\}_i^T \{\phi_B\}_j \right|^2}{(\{\phi_A\}_i^T \{\phi_A\}_i)(\{\phi_B\}_j^T \{\phi_B\}_j)} \quad (1)$$

Zero values indicate the absence of a relationship's consistency, while values equal to unity indicate the presence of a relationship's consistency. The MAC matrix is constructed using all the i and j modal vectors from the two sets of mode shapes, with the matrix dimensions being proportional to the number of mode shapes considered. The current research considers a total of ten modes. As a result, the MAC matrix is 10×10 .

Table 5 Number of selected points and their elevations relative to the dam bottom and Table 6 Calculation results of the MAC matrix for determining the optimal point in various scenarios.

The closer the diagonal elements of the MAC matrix are to one and the off-diagonal elements to zero, the more logically consistent the two sets of obtained responses are. The highest point on the dam crest (point no. 1) is selected as the first optimal location for the first sensor in this study by calculating the MAC matrix. The second optimal point is selected in this manner to maximize the linear independence of the mode shapes. After determining the first point, the optimal value of the following matrix is calculated as follows:

$$MAC(1, j) \quad j = 1, 2, \dots, n \quad (2)$$

Table 5 Number of selected points and their elevations relative to the dam bottom

DM1								
Point No.	1	2	3	4	5			
Elevation (m)	219	211	199	187	175			
Point No.	6	7	8	9	10			
Elevation (m)	161	148	135	123	111			
Point No.	11	12	13	14	15			
Elevation (m)	99.4	87.5	75.3	63.4	51.6			
Point No.	16	17	18	19	20			
Elevation (m)	39.8	27.8	15.9	3.97	0			
DM2								
Point No.	1	2	3	4	5	6	7	8
Elevation (m)	201	201	189	174	159	145	130	115
Point No.	9	10	11	12	13	14	15	16
Elevation (m)	101	86	71	56	41	26	12	0

In the above expression above, n denotes the candidate number of points for the optimal location of sensors. Following the calculation of the MAC matrix, each matrix's most significant off-diagonal element can be calculated using the following expression:

$$MAC\{Non - Diag[MAC(1, j)]\} \quad j = 1, 2, \dots, n \quad (3)$$

Following this, the element with the lowest value is selected from each matrix's largest off-diagonal elements, which indicates the point at which the modes have the most significant linear independence.

As shown in Fig. 8, a sample of the matrices was obtained from the MAC method used to determine the optimal point in scenario no. 1 in the x-direction.

Figs. 9 to 12 depict the optimal locations for sensors to receive the maximum data of the structure mode shapes in the x and y directions, respectively.

5 Proposed equation for optimal location of sensors

In this study, once finished with calculating the modes of healthy and damaged dams, all outputs related to the mid points as well as the ones on both sides of the dam were extracted. Finally, the following equation was used to obtain the difference in displacement between the healthy and damaged dam modes at different damage percentages. The percent displacement difference between the two dams was obtained via the following equation. This equation is based on the displacement difference between the healthy and damaged dams.

$$e_{\phi}^{i,j} = \left| \frac{\phi^{i,j} - \phi_d^{i,j}}{\phi^{i,j}} \right| \times 100 \quad (4)$$

Table 6 Calculation results of the MAC matrix for determining the optimal point in various scenarios

DM1		
Scenario	Optimal location considering the modes in the x-direction	Optimal location considering the modes in the y-direction
1	1, 5, 7, 9, 10, 14	1, 7, 10, 11, 12
2	1, 2, 3, 5, 7, 9, 10, 11, 15	1, 7, 8, 9, 10, 15
3	1, 3, 5, 7, 9, 10, 14	1, 8, 9, 10, 11
DM2		
Scenario	Optimal location considering the modes in the x-direction	Optimal location considering the modes in the y-direction
1	1, 3, 4, 5, 6, 7, 10, 14	1, 4, 5, 7, 10, 14
2	1, 4, 6, 7, 8, 9, 10, 11, 12	1, 6, 7, 8, 10, 11, 12
3	1, 3, 6, 8, 10, 11	1, 6, 8, 10, 11

In this equation, $e_{\phi}^{i,j}$ is the percent difference in displacement between the two structures in the same mode at point j , $\phi^{i,j}$ denotes the displacement of the healthy

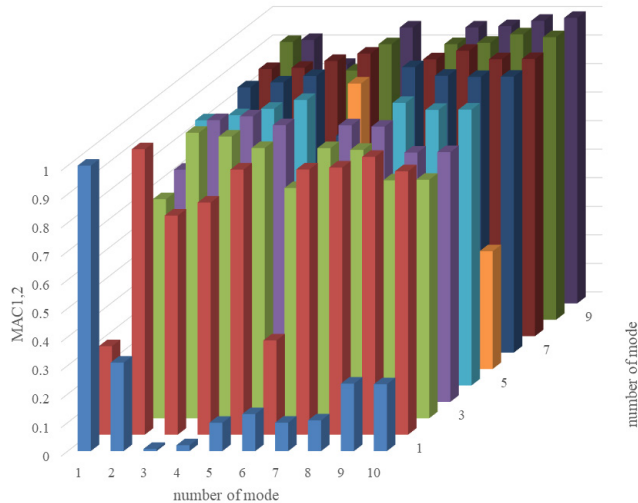


Fig. 8 A sample of the MAC matrix calculations corresponding to the second optimal point in scenario no. 1, considering the modes in the x-direction

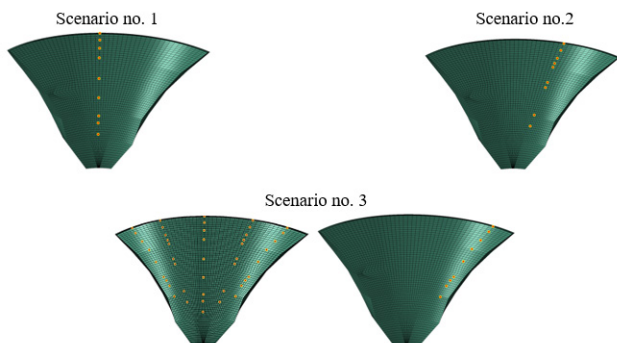


Fig. 9 DM1 optimal sensor locations to obtain the maximum data on the mode shapes in the x-direction for various scenarios

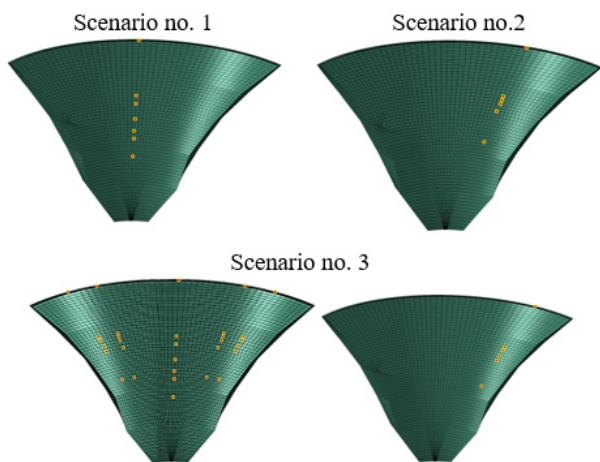


Fig. 10 A. DM2 optimal sensor locations to obtain the maximum data on the mode shapes in the y-direction for various scenarios

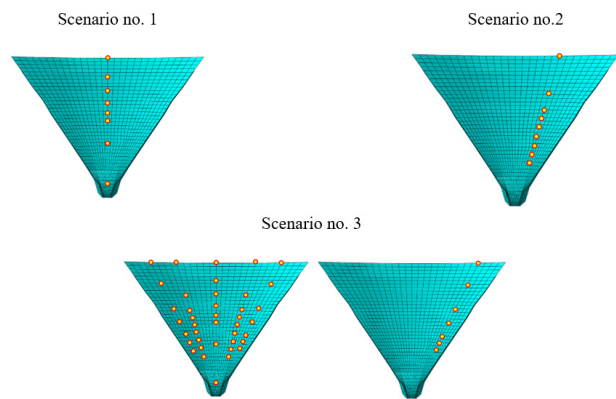


Fig. 11 DM1 optimal sensor locations to obtain the maximum data on the mode shapes in the x-direction for various scenarios

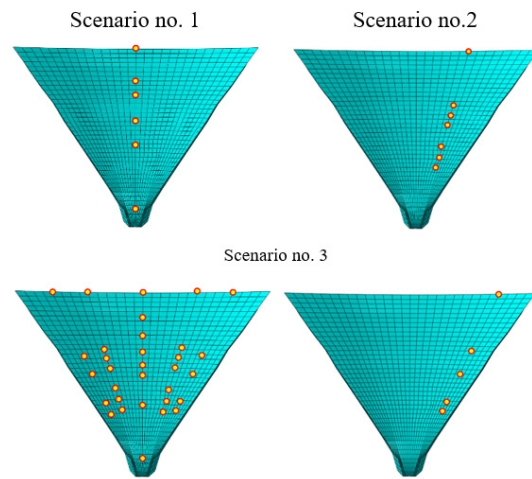


Fig. 12 DM2 optimal sensor locations to obtain the maximum data on the mode shapes in the y-direction for various scenarios

structure in mode i , and $e_d^{i,j}$ refers to displacement of the damaged structure in mode i .

In this research, investigating the displacements along x and y axes, it was observed that the displacement along y -axis was negligible in majority of modes, leading to insignificant displacement differences in this direction. Accordingly, investigations were focused on the x -axis where the differences, and hence the sensitivity, were higher.

Upon a curve fitting, the following relationship was obtained for explaining the association between relative height and damage percentage for all points. This relationship was obtained by overlapping more than 90% of the data points. All calculations were conducted in MATLAB. The following equation was obtained under Scenario I:

The proposed equation for one-eighths of the dam length from the banks (Scenario I, Fig. 13.) at 100% water level is as follows:

$$\begin{aligned}
 e_{\phi}^{i,j} = & 94.2 \sin(-0.184x - 0.0052) + 3.49 \sin(7.64x - 1.23) \\
 & + 2 \sin(38.19x - 3.306) + 2.19 \sin(25.85x - 1.19) \\
 & + 1.338 \sin(61.83x + 1.5) + 2.89 \sin(-28.23x - 1.27) \\
 & + 2.25 \sin(14.42x + 1.139)
 \end{aligned}
 \tag{5}$$

Upon a curve fitting, the following relationship was obtained for explaining the association between relative height and damage percentage for all points. This relationship was obtained by overlapping more than 90% of the data points. All calculations were conducted in MATLAB. The following equation was obtained under Scenario II (Fig. 14):

$$\begin{aligned}
 e_{\phi}^{i,j} = & 213.4 \sin(0.78x + 0.43) + 3.98 \sin(9.43x - 2.23) \\
 & + 2.42 \sin(11.26x - 2.53) + 194.2 \sin(0.84x - 2.74) \\
 & + 8.572 \sin(4.19x + 2.98) + 7.52 \sin(4.615x - 0.63) \\
 & + 2.76 \sin(7.06x - 1.53)
 \end{aligned}
 \tag{6}$$

For Scenario III (Fig. 15), a similar procedure to that implemented for Scenarios I and II was undertaken.

The proposed equation for one-four of the dam length from the banks (Scenario I) at 100% water level is as follows:

$$\begin{aligned}
 e_{\phi}^{i,j} = & 12.84 \sin(2.54x - 0.19) + 1.29 \sin(21.79x - 6.785) \\
 & + 1.36 \sin(31.39x - 4.45) + 3.24 \sin(12.36x + 2.304) \\
 & + 0.37 \sin(63.97x + 3.07) + 0.37 \sin(54.22x + 0.14) \\
 & + 1.079 \sin(47.62x - 2.646)
 \end{aligned}
 \tag{7}$$

Considering the plots, the peaks indicate the points that correspond to the maximum difference between healthy and damage modes, making the best positions for installing the sensors for maximizing the information acquisition and reporting. The following tables (Tables 7–8) provide a list of the optimal sensor positions as per MAC and the proposed relationship. These tables refer to the first dam, i.e., Dam DM1. All values under different scenarios are indicated on the basis of relative heights with reference to the dam height.

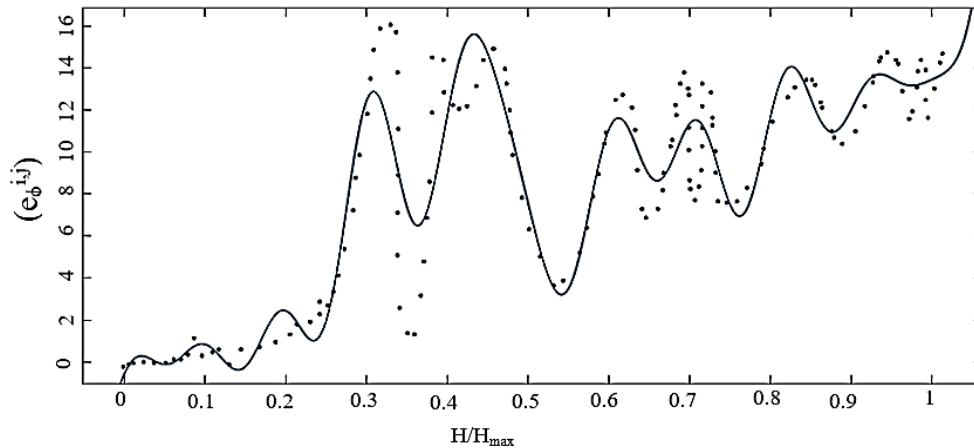


Fig. 13 Curve fitting to all calculated points with different damage percentages over Dam DM1 under Scenario I.

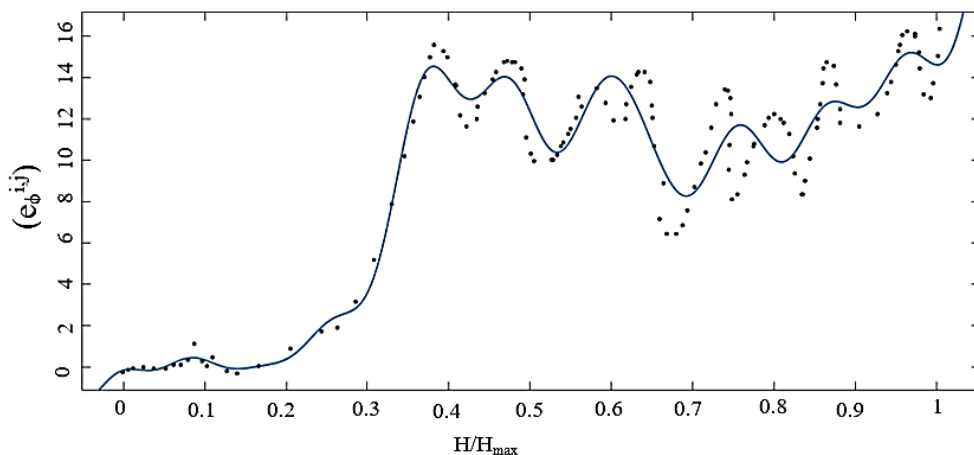


Fig. 14 Curve fitting to all calculated points with different damage percentages over Dam DM1

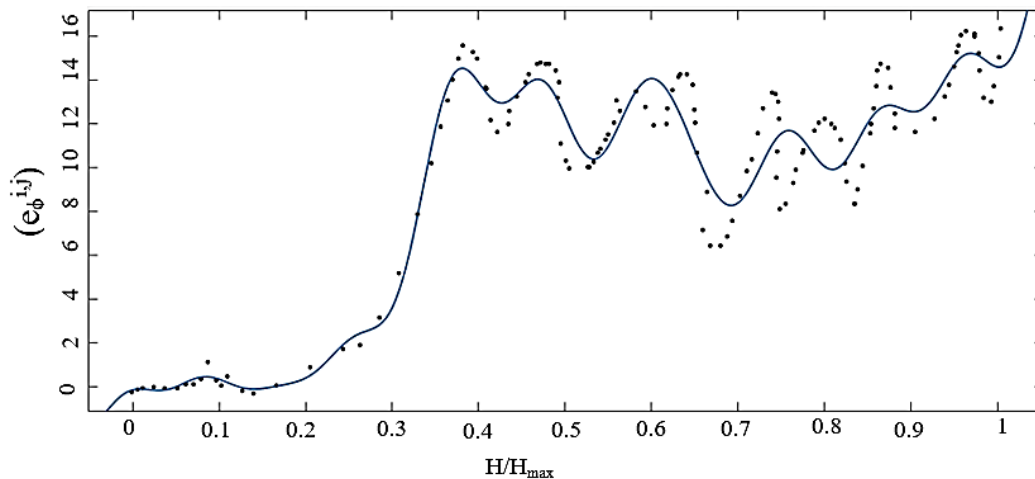


Fig. 15 Curve fitting to all calculated points with different damage percentages over Dam DM1 under Scenario I. (water level 100 percent)

Investigating the optimal positions on the studied dam under Scenarios II and III based on the MAC, we observed that distribution of the optimally-positioned sensors extends from a relative height of 0.32 up to the dam crown. Indeed, the points at relative heights of 1 (the dam crown), 0.95, 0.64, 0.41, and 0.32 were optimal under all of the three scenarios. Optimal sensor positions are compared between the MAC and the proposed equation in Table 9.

Considering the best positions for sensors as per MAC and the peaks of the fitted curve based on the proposed equation, it is evident that these two sets of positions closely resemble one another, being within 5% of one another. In the proposed methodology, one should further consider a constraint for point selection to ensure that the selected positions fall in a relative height of at least 0.3. Therefore, the following relationships can be developed to give the optimal sensor position based on the proposed equation:

According to the proposed equation, best sensor positions under Scenario I (i.e., one-eighths of dam length from banks) are as follows:

Table 7 Optimal positions for the sensors in x-direction of the structure under different scenarios, as per MAC, in Dam DM1

Scenarios I one-eighths	Scenarios II half dam	Scenarios III one-four
1	1	1
0.95	0.95	0.95
0.81	0.86	0.86
0.68	0.77	0.82
0.64	0.64	0.80
0.52	0.52	0.66
0.48	0.41	0.64
0.41	0.36	0.41
0.32	0.32	0.32

$$\begin{aligned}
 (e_{\phi}^{i,j})' &= 0 \\
 &17.3394.2 \cos(-0.184x - 0.0052) + 26.59 \cos(7.64x - 1.23) \\
 &+ 78.38 \cos(38.19x - 3.306) + 56.61 \cos(25.85x - 1.19) \\
 &+ 82.73 \cos(61.83x + 1.5) + 81.58 \cos(-28.23x - 1.27) \\
 &+ 32.445 \cos(14.42x + 1.139) = 0
 \end{aligned} \tag{8}$$

Under Scenario II, the proposed equation gives the following best sensor positions:

$$\begin{aligned}
 (e_{\phi}^{i,j})' &= 0 \\
 &166.45 \cos(0.78x + 0.43) + 37.53 \cos(9.43x - 2.23) \\
 &+ 27.25 \cos(11.26x - 2.53) + 163.13 \cos(0.84x - 2.74) \\
 &+ 35.92 \cos(4.19x + 2.98) + 34.7 \cos(4.615x - 0.63) \\
 &+ 19.49 \cos(7.06x - 1.53) = 0
 \end{aligned} \tag{9}$$

Under Scenario III, the proposed equation gives the following best sensor positions:

Table 8 Optimal positions for the sensors in x-direction of the structure under different scenarios, as per MAC, in Dam DM2

(H/Hmax) Relative height		
Scenarios I	Scenarios II	Scenarios III
1	1	1
0.95	0.95	0.95
0.81	0.86	0.86
0.68	0.77	0.82
0.64	0.64	0.8
0.52	0.52	0.66
0.48	0.41	0.64
0.41	0.36	0.41
0.32	0.32	0.32

Table 9 Comparison of proposed equation with MAC in terms of optimal positions for the sensors in x-direction of the structure under different scenarios in Dam DM1

Relative height (H/Hmax)					
Scenarios I		Scenarios II		Scenarios III	
MAC	Proposed relationship	MAC	Proposed relationship	MAC	Proposed relationship
1	1	1	1	1	1
0.95	0.95	0.95	0.96	0.95	0.97
-	0.86	-	0.92	0.86	0.86
0.81	0.81	0.86	0.84	0.82	0.82
-	0.78	-	0.77	0.80	0.75
-	0.71	0.73	0.71	0.66	0.69
0.68	0.66	0.64	0.63	0.64	0.62
0.64	0.62	0.52	0.52	-	0.53
0.52	0.54	-	0.43	-	0.48
0.48	0.45	0.41	0.41	0.41	0.41
0.41	0.38	0.36	0.34	0.32	0.38
0.32	0.32	0.32			0.12
	0.23				0.08
	0.19				
	0.15				

Table 10 Comparison of the proposed relation of the optimal location of sensors and the MAC method in the X direction for the DM2 dam in different scenarios

Relative height (H/Hmax)					
Scenarios I		Scenarios II		Scenarios III	
MAC	Proposed relationship	MAC	Proposed relationship	MAC	Proposed relationship
1	1	1	1	1	1
0.91	0.95		0.96		0.97
0.86	0.86		0.92	0.91	0.86
	0.81		0.84	0.82	0.82
0.76	0.78	0.76	0.77		0.75
0.71	0.71	0.71	0.71	0.68	0.69
	0.66	0.62	0.63	0.57	0.62
	0.62	0.57		0.53	0.53
0.57	0.54	0.52	0.52	0.48	0.48
	0.45	0.48			0.41
	0.38	0.43	0.43		0.38
	0.32	0.38	0.41		0.12
0.24	0.23	0.31	0.34		0.08
	0.19				
	0.15				

$$(e^{i-j})' = 0$$

$$32.61 \cos(2.54x - 0.19) + 28.11 \cos(21.79x - 6.785) + 42.69 \cos(31.39x - 4.45) + 40.04 \cos(12.36x + 2.304) + 17.62 \cos(47.62x - 2.646) = 0 \tag{10}$$

In order to investigate the precision and accuracy of the results of the proposed equation, optimal sensor positions were calculated for Berke Dam in Turkey with the specifications given in Fig. 2, with the results presented in Table 10. The positions were once more calculated by the MAC, and the table further compares the results of the two methodologies.

Comparing the results on the Berke Dam by using the MAC and the proposed methodology under the three scenarios, it was observed that the two techniques returned very close outcomes with a maximum difference of 6%, indicating good agreement of the results. Nevertheless, the proposed methodology identifies more positions for sensors, which can be utilized should a higher level of accuracy be required for a particular project.

The present study is aimed at proposing a fast, inexpensive, and reliable method for locating sensors to acquire information for dam monitoring and damage prevention.

6 Conclusions

In the present research, the modal assurance criterion was used to analyze data from a modal analysis conducted on a large double curvature arch dam in three scenarios. Identify potential damage points, and the optimal locations for sensors were identified and presented. Overall, the research's most significant findings can be summarized as follows:

- The elevations for placing sensors and sensitive points in each of the three defined scenarios are nearly identical.
- On all elevations, the optimal location for sensor installation in all scenarios was the dam crest. As a result, the dam crest is a critical and sensitive location that should be considered.
- Along with the point specified on the dam crest, points in the middle of the dam body are also desirable locations for the sensors.
- When the optimal points were located using the modes at the x-direction, the ratio of the optimal point height to the dam height (from the bottom) was 0.8, 0.68, 0.56, 0.51, and 0.29 in scenario no.1. This ratio indicates that the middle portion of the dam body between 0.51 and 0.68 includes the optimal x-direction points in scenario no.1. The investigation of scenario no. 2 revealed that the optimal point height to

the dam height (from the bottom) ratios were 0.96, 0.91, 0.8, 0.68, 0.56, 0.51, 0.45, and 0.24, respectively. As demonstrated in this scenario, the optimal points at the top and middle portions are critical. The ratio of optimal point height to dam height (from the bottom) was 0.96, 0.91, 0.80, 0.68, 0.56, 0.51, and 0.29 in the third scenario. It is worth noting that the optimal points in this scenario are nearly identical to the optimal points in the second scenario, implying that the results are nearly identical.

- When the optimal points were located using the modes at the y-direction, the ratio of the optimal point height to the dam height (from the bottom) was 0.68, 0.51, 0.45, and 0.40 in scenario no.1. This ratio indicates that the middle portion of the dam body between 0.40 and 0.68 contains the optimal points for the y-direction modes. Investigating scenario no. 2 in the y-direction revealed that the ratio of optimal point height to dam height (from the bottom) was 0.68, 0.61, 0.56, 0.51, 0.24, respectively. As demonstrated in this scenario, the optimal points in the middle portion are also critical. In the third scenario, the optimal point height was equal to the dam height (from the bottom) by a factor of 0.62, 0.56, 0.51, and 0.24, respectively. It is noted that the optimal points in this scenario are nearly symmetrical concerning the optimal points in the second scenario, which produces nearly identical results.
- Analyses of the results in both the x and y directions revealed that the points located on the dam crest are critical for dam control because they are located in an area critical for dam control. As the client determines the number of sensors to be used, one could be installed one on the dam crest and the remaining sensors distributed throughout the body, as shown in the relevant table.

- The points closest to the lower portion of this dam have a high sensitivity. At the points corresponding to the right and left portions, it is observed that the middle points are more sensitive. Where damage occurs at the upper, middle, and lower portions, the middle points exhibit a greater sensitivity.
- Additionally, when examining the middle points, it is observed that the points closest to the dam's upper portion have a higher sensitivity than the points closest to the dam's base.
- When all points are investigated, it is observed that points 1, 6, and 10 have a similar sensitivity to all scenarios, and their sensitivity is significant.
- Point 8 is critical in both the left and right corner scenarios, and it is significant and sensitive in both scenarios.
- Following an examination of the data presented in this study, it was determined that the second and fifth modes are more sensitive than the others. The difference is calculated using the modal assurance criterion method. However, the proposed criterion identifies the sensitive modes first and then the sensitive points for sensor installation. Both the proposed method and the MAC method demonstrate that the points in the middle of the dam body up to its crest are the most sensitive and that as we approach the lower portion of the dam, the difference between healthy and damaged dam displacements decreases.
- By selecting the second and fifth modes as the dominant modes, a relationship between dam height and the ratio of healthy-dam displacement to damaged-dam displacement could be derived.
- The relationship proposed in this paper is highly compatible with the MAC method, which can be used more reliably in its place.

References

- [1] Farrar, C. R., Worden, K. "Title of the content on page 27-70", In: Structural Health Monitoring: A Machine Learning Perspective, Wiley, 2012, pp. 27–70. ISBN:9781119994336
<https://doi.org/10.1002/9781118443118>
- [2] Dawson, B. "Vibration condition monitoring techniques for rotating machinery", The Shock and Vibration Digest, 8(12), pp. 3–8, 1976.
<https://doi.org/10.1177/058310247600801203>
- [3] U.S. Army Corps of Engineers "Distribution Restriction Statements, Distribution Statement A: Approved for public release. Distribution is unlimited", Department of Defense, USA, 1994. [online] Available at: <https://www.dodcuil.mil/Distribution-Statements/>
- [4] Cawley, P., Adams, R. D. "The location of defects in structures from measurements of natural frequencies", The Journal of Strain Analysis for Engineering Design, 14(2), pp. 49–57, 1979.
<https://doi.org/10.1243/03093247V142049>
- [5] West, W. M. "Illustration of the use of modal assurance criterion to detect structural changes in an orbiter test specimen", In: Proceedings in Air Force Conference on Aircraft Structural Integrity Program, U.S. Air Force, 1986, Document ID 19870041253. [online] Available at: <https://ntrs.nasa.gov/citations/19870041253>
- [6] Ghasemi, M. R., Ghiasi, R., Varae, H. "Probability-Based Damage Detection of Structures Using Kriging Surrogates and Enhanced Ideal Gas Molecular Movement Algorithm", In: World Congress of Structural and Multidisciplinary Optimisation, Advances in Structural and Multidisciplinary Optimisation, Braunschweig, Germany, 2017, pp. 1657–1674. ISBN 978-3-319-67987-7
https://doi.org/10.1007/978-3-319-67988-4_124
- [7] Zhu, K., Gu, C., Qiu, J., Liu, W., Fang, C., Li, B. "Determining the Optimal Placement of Sensors on a Concrete Arch Dam Using a Quantum Genetic Algorithm", Journal of Sensors, 2016, 2567305, 2016.
<https://doi.org/10.1155/2016/2567305>

- [8] Chen, B., Huang, Z., Zheng, D., Zhong, L. "A hybrid method of optimal sensor placement for dynamic response monitoring of hydro-structures", *International Journal of Distributed Sensor Networks*, 13(5), pp. 1–12, 2017.
<https://doi.org/10.1177/1550147717707728>
- [9] Esmailzadeh, S., Ahmadi, H., Hosseini, S. A. "Damage detection of concrete gravity dams using Hilbert-Huang method", *Journal of Applied Engineering Sciences*, 8(2), pp. 7–16, 2018.
<https://doi.org/10.2478/jaes-2018-0012>
- [10] Shi, B., Li, M., Song, L., Zhang, M., Shen, Y. "Deformation coordination analysis of CC-RCC combined dam structures under dynamic loads", *Water Science and Engineering*, 13(2), pp. 162–170, 2020.
<https://doi.org/10.1016/j.wse.2020.07.001>
- [11] Zhang, Y., Feng, X., Fan, Z., Hou, S., Zhu, T., Zhou, J. "Experimental investigations on seismic damage monitoring of concrete dams using distributed lead zirconate titanate sensor network", *Advances in Structural Engineering*, 20(2), pp. 170–179, 2017.
<https://doi.org/10.1177/1369433216660002>
- [12] Hamidian, D., Salajegheh, E., Salajegheh, J. "Irregular continuum structures damage detection based on wavelet transform and neural network", *KSCE Journal of Civil Engineering*, 22, pp. 4345–4352, 2018.
<https://doi.org/10.1007/s12205-018-1470-z>
- [13] Gomes, G. F., Purcino Pereira, J. V. "Sensor placement optimization and damage identification in a fuselage structure using inverse modal problem and firefly algorithm", *Evolutionary Intelligence*, 13, pp. 571–591, 2020.
<https://doi.org/10.1007/s12065-020-00372-1>
- [14] Hornarbakhsh, A., Nagayama, T., Rana, S., Tominaga, T., Hisazumi, K., Kanno, R. "Damage identification of belt conveyor support structure using periodic and isolated local vibration modes", *Smart Structures and Systems*, 15(3), pp. 787–806, 2015.
<https://doi.org/10.12989/sss.2015.15.3.787>
- [15] Cotae, P., Yalamanchili, S., Chen, C. L. P. "Optimization of sensor locations and sensitivity analysis for engine health monitoring using minimum interference algorithms", 2007 IEEE International Conference on System of Systems Engineering, San Antonio, TX, USA, 2007, pp. 1-6. ISBN:1-4244-1159-9
<https://doi.org/10.1109/SYSESE.2007.4304321>
- [16] Li, B., Ou, J., Zhao, X., Li, D. "Optimal Sensor placement in health monitoring system of Xinghai Bay bridge", presented at the 6th International Workshop on Advanced Smart Materials and Smart Structures Technology, Dalian, China, July, 25–26, 2011.
- [17] Yi, T.-H., Li, H.-N., Gu, M. "Optimal sensor placement for health monitoring of high-rise structure based on genetic algorithm", *Mathematical Problems in Engineering*, 2011, 395101, 2011.
<https://doi.org/10.1155/2011/395101>
- [18] Vegrzyn, R., Fonseca, B. J. B. "Optimizing Sensor Locations to Improve the Worst Case Detection Performance of Sensor Detection Systems", presented at: 55th Annual Conference on Information Sciences and Systems (CISS), Baltimore, MD, USA, March, 24–26, 2021.
<https://doi.org/10.1109/CISS50987.2021.9400220>
- [19] Shi, Z. Y., Law, S. S., Zhang, L. M. "Optimum Sensor Placement for Structural Damage Detection", *Journal of Engineering Mechanics*, 126(11), pp. 1173–1179, 2000.
<https://doi.org/10.2174/1872212113666190110124551>
- [20] Han, B., Geng, F., Dai, S., Gan, G., Liu, S., Yao, L. "Statistically optimized back-propagation neural-network model and its application for deformation monitoring and prediction of Concrete-Face Rockfill Dams", *Journal of Performance of Constructed Facilities*, 34(4), 04020071, 2020.
[https://doi.org/10.1061/\(ASCE\)CF.1943-5509.0001485](https://doi.org/10.1061/(ASCE)CF.1943-5509.0001485)
- [21] Altunisik, A. C., Sevim, B., Sunca, F., Okur, F. Y. "Optimal sensor placements for system identification of concrete arch dams", *Advances in Concrete Construction*, 11(5), pp. 397–407, 2021.
<https://doi.org/10.12989/acc.2021.11.5.397>
- [22] Gomes, G. F., Pereira, J. V. P. "Sensor placement optimization and damage identification in a fuselage structure using inverse modal problem and firefly algorithm", *Evolutionary Intelligence*, 13, pp. 571–591, 2020.
<https://doi.org/10.1007/s12065-020-00372-1>
- [23] Gomes, G. F., da Cunha Jr., S. S., da Silva Lopes Alexandrino, P., de Sousa, B. S., Ancelotti Jr., A. C. "Sensor placement optimization applied to laminated composite plates under vibration", *Structural and Multidisciplinary Optimization*, 58, pp. 2099–2118, 2018.
<https://doi.org/10.1007/s00158-018-2024-1>
- [24] Gomes, G. F., de Almeida, F. A., da Silva Lopes Alexandrino, P., da Cunha Jr., S. S., de Sousa, B. S., Ancelotti Jr., A. C. "A multiobjective sensor placement optimization for SHM systems considering Fisher information matrix and mode shape interpolation", *Engineering with Computers*, 35, pp. 519–535, 2019.
<https://doi.org/10.1007/s00366-018-0613-7>
- [25] Hernandez, W., Viviescas, A., Riveros-Jerez, C. A. "Verifying of the finite element model of the bridge based on the vibration monitoring at different stages of construction", *Archives of Civil Engineering*, 66(1), pp. 25–40, 2020.
<https://doi.org/10.24425/ace.2020.131772>
- [26] Mehboob, S., Zaman Khan, Q. U., Ahmad, S. "Numerical study for evaluation of a vibration based damage index for effective damage detection", *Bulletin of the Polish Academy of Sciences, Technical Sciences*, 68(6), pp. 1443–1456, 2020.
<https://doi.org/10.24425/bpasts.2020.134651>
- [27] Hellgren, R., Gasch, T. "Influence of Fluid Structure Interaction on a Concrete Dam during Seismic Excitation", In: *Second International Dam World Conference*, Lisbon, Portugal, 2014, pp. 333–342.
- [28] Goldgruber, M., Zenz, G. "Theme A. Fluid Structure Interaction Arch Dam – Reservoir at Seismic loading", In: *Proceedings of the 12th International Benchmark Workshop on Numerical Analysis of Dams*, Graz, Austria, 2013, pp. 13–177.
- [29] Allemang, R. J. "The modal assurance criterion - Twenty years of use and abuse", *Sound and Vibration*, 37(8), pp. 14–21, 2003.